XXVIII. NEUROLOGY[*]

L. Stark	Y. Okabe	J. Simpson
S. Asano	M. Okajima	I. Sobel
F. H. Baker	R. C. Payne	S. F. Stanton
C. A. Finnila	N. Perrin	J. Stark
G. Gottlieb	Julia H. Redhead	Y. Takahashi
H. T. Hermann	Helen E. Rhodes	E. Van Horn
J. C. Houk	V. Sanchez	L. A. M. Verbeek
R. Howland	A. Sandberg	P. A. Willis
G. P. Nelson	P. R. Samson	L. R. Young
C. Northrup	G. Sever	W. Zapol

RESEARCH OBJECTIVES

The aim of our work is to apply the concepts of communication and control theory to an analysis of neurological servomechanisms. The group is composed of neurologists, mathematicians, and electrical engineers. Our research endeavors span a wide field that includes experiments on human control mechanisms, mathematical methods for analysis of nonlinear systems, including simulation, clinical studies using on-line digital-computer techniques, neurophysiology of simple invertebrate receptors, and adaptive pattern-recognition techniques using computers.

L. Stark

A. THE DYNAMIC CHARACTERISTICS OF A MUSCLE MODEL USED IN DIGITAL-COMPUTER SIMULATION OF AN AGONIST-ANTAGONIST MUSCLE SYSTEM IN MAN

1. Physiological Studies

Fenn and Marsh[1] first showed that the dynamic characteristics of a maximally stimulated, shortening muscle of a frog could be approximated by an experimental relationship between the load on a muscle and the maximum velocity of the muscle. In 1938, Hill[2] showed in a thermodynamic study of frog muscle that the force-velocity relationship could be approximated very closely by the equation

$$(v+b)(P+a) = (P_o+a) b = \text{constant},$$

where a and b are constants that are dependent on the particular muscle, P is load, v is velocity, and P_o is isometric tension. When experiments were extended to the lengthening, as well as the shortening, muscle, Hill's equation was shown to fail. Katz found a steep linear relationship between muscle opposition force and lengthening velocity.[3] See Fig. XXVIII-1.

Ten years later, Wilkie[4] repeated Hill's experiments for the shortening muscle in
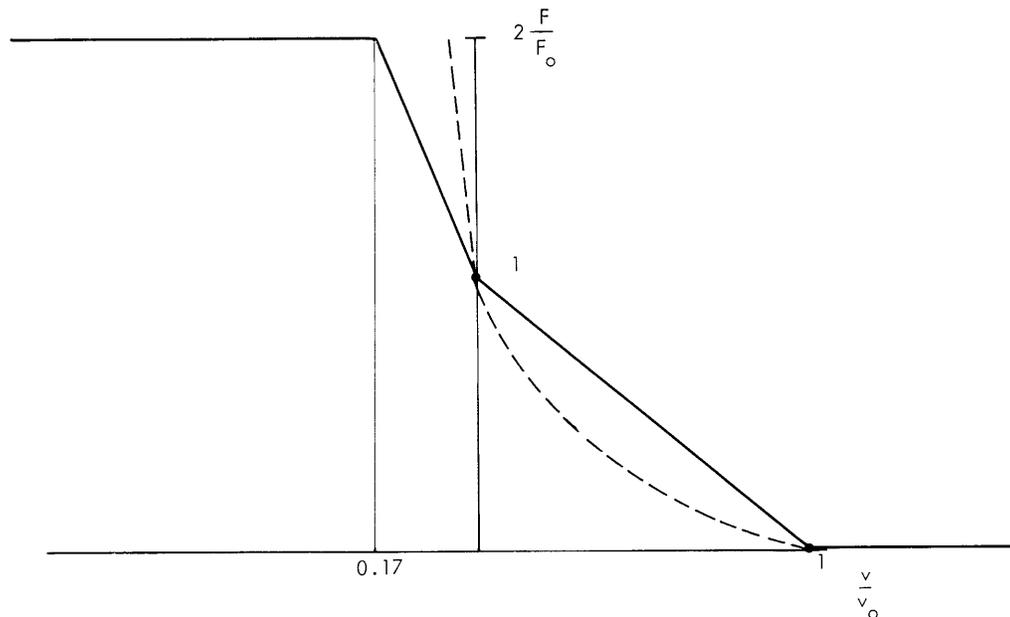
Fig. XXVIII-1. Comparison of BIOSIM model with experiment. The solid curve shows the force-velocity relationship of the BIOSIM model; the dashed curve, the force-velocity relationship of frog muscle as obtained by Katz. For frog muscle P_o = 0. 1 kg, v_o = 4 cm/sec.

the human arm by using subjects who were directed to exert maximal voluntary effort. His results fit Hill's equation after he corrected for the inertia of the arm. These data were most effective in our approximation of a muscle model for digital-computer simulation.

2. BIOSIM Model of Muscle Dynamics

The primary purpose of building a muscle model for BIOSIM was not to investigate the mathematical characteristics of Hill's model, but rather to investigate the behavior of a complete agonist-antagonist muscle system. Therefore, some very simple approximations to the accurate physiological model were adequate for this work. The force-velocity relationship for excessive velocity of both the lengthening and the shortening muscle have not been determined physiologically. When these critical velocities are exceeded, one thing or a combination of a variety of things may happen. The reasons for selecting the model shown in Fig. XXVIII-2 are explained below.

Within the critical velocities, straight-line approximations are made. We estimated P_o (the maximum isometric force) and v_o (the maximum velocity with no load) by using the parameters in Wilkie's paper[4] and actual estimates on human subjects. The slope of the straight line representing lengthening, B_L, is made six times greater than that for shortening, B_s. The following parameters were selected:

$$P_O = 100 \text{ kg}$$

$$v_O = 0.01 \text{ m/sec}$$

$$B_S = -10,000 \, \frac{\text{kg} - \text{sec}^2}{\text{m}}$$

$$B_L = -60,000 \, \frac{\text{kg} - \text{sec}^2}{\text{m}}$$

If a muscle is shortened at a velocity greater than that at which it is capable of shortening itself, it exerts no force. Thus P is zero for velocities greater than v_O. When a muscle is stretched more rapidly than its critical stretching velocity, several
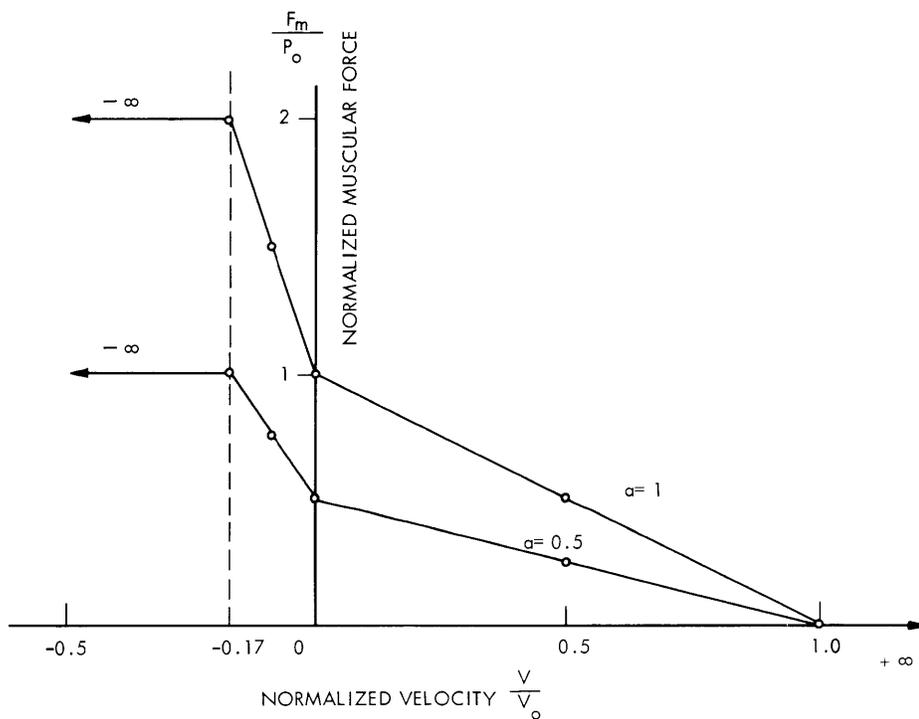

Fig. XXVIII-2. Force-velocity relationship of BIOSIM model. (a = 1, maximal stimulation; a = 0.5, half-maximal stimulation.)

things may happen. A phenomena called "slipping" or "yielding" occurs first. Hill[5] wrote: "Under a load rather greater than it can bear an active muscle lengthens slowly, under a considerably greater load it 'gives' or 'slips.' We can regard the first process as 'reversible' in the thermodynamic sense, the second as largely 'irreversible.'"

311

Katz[3] found that contractile structures of a muscle may be damaged if its velocity of lengthening is increased rapidly while the muscle is active. Normally, the Golgi tendon organ (a tension-sensing device) reflexly causes the muscle to relax before this damage occurs.
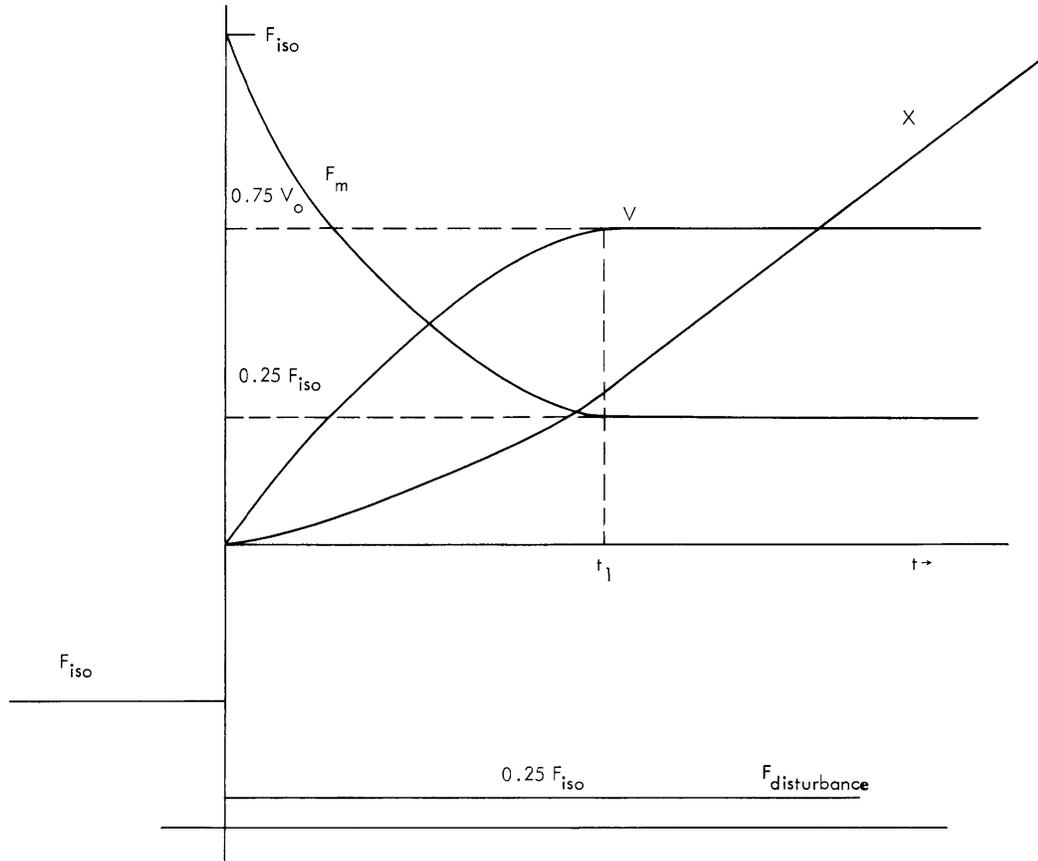

Fig. XXVIII-3. The experiment performed with the BIOSIM model. F_m is the total force exerted by the muscle, x is muscle displacement, v is muscle velocity, excitation is maximal. The time t_1 was necessary for the model to overcome inertia and reach constant velocity.

It is expected that future simulation will seldom operate in the critical region. Thus a compromise between complete relaxation and increased resistance caused by slipping is used. For velocities of lengthening which are greater than critical, the BIOSIM model saturates at 2P. See Fig. XXVIII-1.

No physiological data are available for muscle stimulation that is less than maximal. It was therefore necessary to speculate. When a muscle is stimulated at half maximum, we assume that the active muscle has the same length, but only one-half the
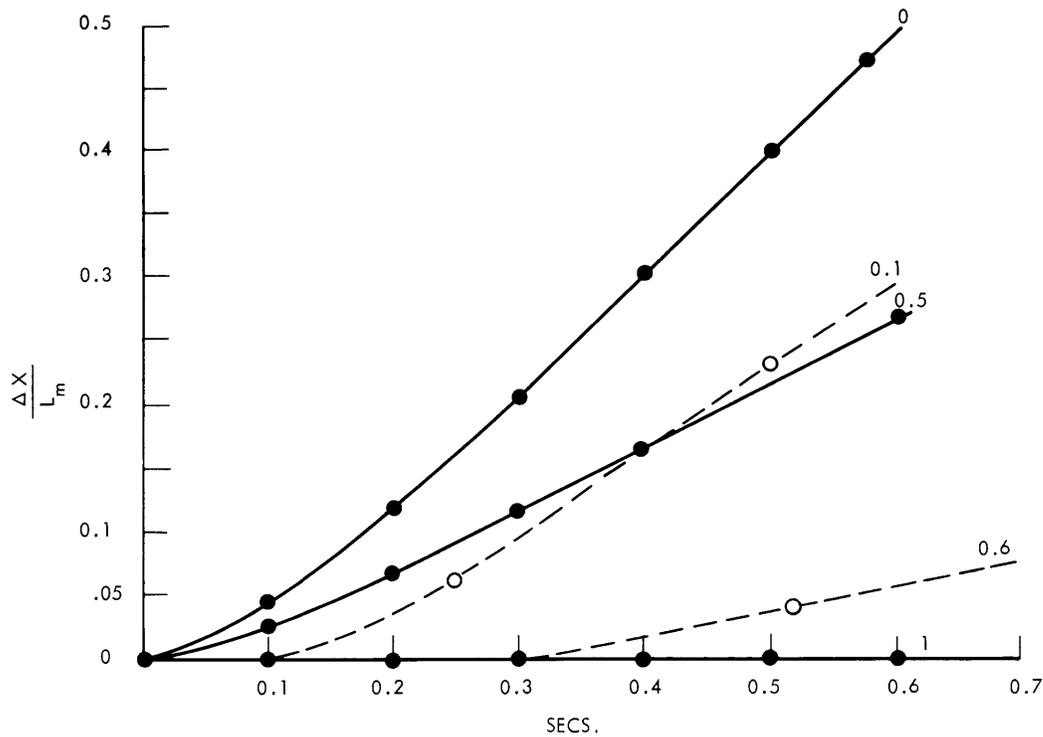
Fig. XXVIII-4. Comparison of BIOSIM model with Fenn and Marsh experiments. The plots show change in length of muscle divided by the length of the muscle vs time. Solid lines represent data from the BIOSIM model; dashed lines show the similar shape obtained by Fenn and Marsh, when normalized stretch and time are corrected to the physiological scale of man. The corrections are suggested by Hill.[7] The parameter noted on the curves is the normalized load, $\dfrac{F_{load}}{F_{iso}}$.

cross-section area, as the fully activated muscle. Therefore, the force output, proportional to cross-section area, is halved while the maximum velocity of shortening, proportional to muscle length, remains constant. These relationships between force and velocity in a half-activated muscle may be obtained by applying the P_o and v_o values for $a = 0.5$ to our original approximations, that is, straight-line relationship and $B_L = 6B_s$. The resultant relationships are shown in Fig. XXVIII-3 and expressed in Eqs. 1 and 2.

$$F_{muscle} = a[P_o + B_s v] \qquad 0 < v < v_o \tag{1}$$

$$F_{muscle} = a[P_o + B_L v] \qquad -\frac{v_o}{6} < v < 0 \tag{2}$$

Figure XXVIII-3 illustrates the model experiment conducted on the 709 computer. Figure XXVIII-4 shows that the model response in displacement has a shape similar to that of a plot of the same variables for frog muscle in the Fenn and Marsh[1] experiments.
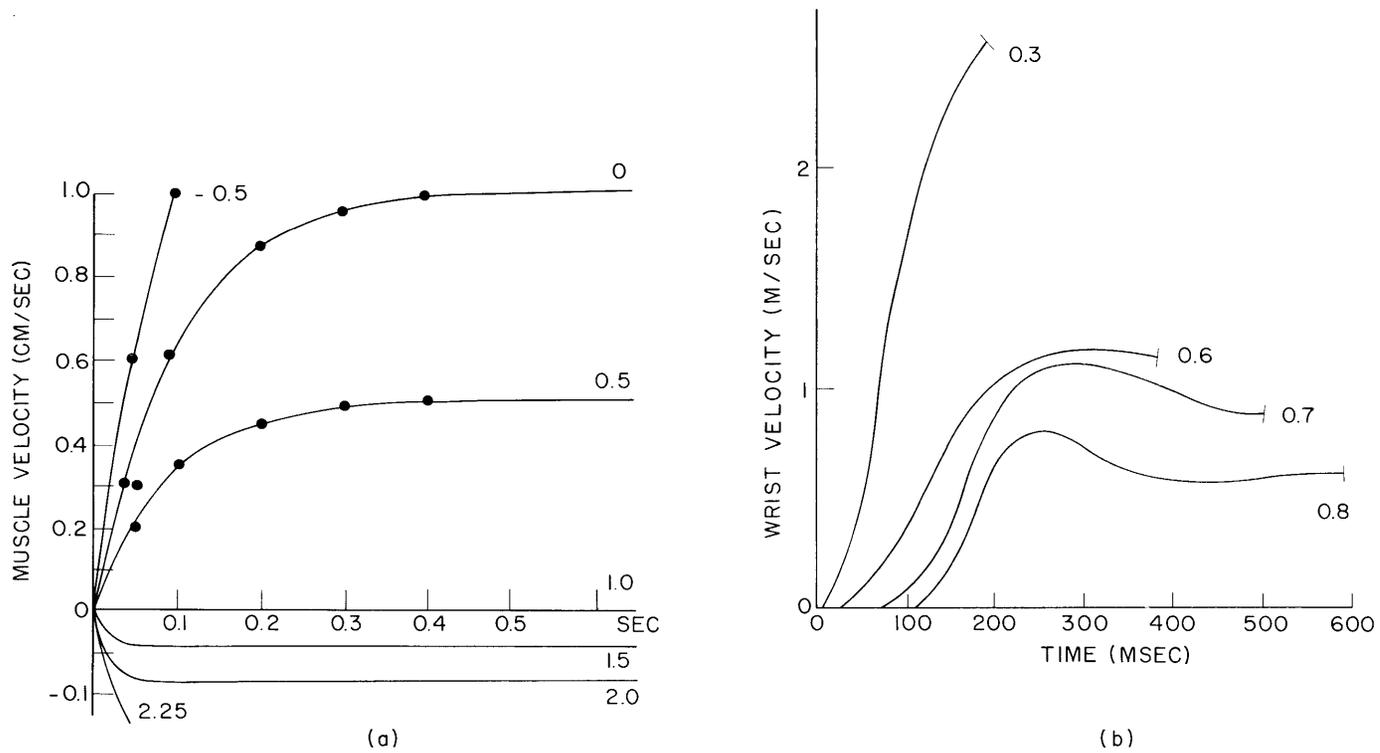
313

Fig. XXVIII-5. Comparison of BIOSIM model with Wilkie's data. The velocity of muscle is plotted as a function of time. As in Fig. XXVIII-4, the parameters are normalized load. (a) BIOSIM data. (b) Wilkie's experimental data.

The dead time in the physiological studies is the time taken for the muscle isometric force to build up to the load force.   Figure XXVIII-5 shows a comparison of velocity versus time with Wilkie's data.[4]

The asymmetrical characteristics become very important in smoothly terminating a rapid voluntary movement.   Asymmetry increases the effective damping over that of a possible symmetrical relationship.   Addition of the postural system (muscle spindle and afferent feedback) as shown by Stark[6] further increases man's power of rapidly damping his motion.   Experiments illustrating the ability of the model to damp without the postural system, and increased ability to damp when the postural system is turned on, should be very interesting.

We thank the Computation Center, M. I. T. , for their services in performing these experiments.

L. Stark, J. Houk, P. A. Willis, J. Elkind

References

1. W. O. Fenn and B. S. Marsh, Muscular force at different speeds of shortening, J. Physiol. 85, 277 (1935).

2. A. V. Hill, The heat of shortening and the dynamic constants of muscle, Proc. Roy. Soc. (London) B126, 136 (1938).

3. B. Katz, The relation between force and speed in muscular contraction, J. Physiol. 96, 45 (1939).

4. D. R. Wilkie, The relation between force and velocity in human muscle, J. Physiol. 110, 249-280 (1950).

5. A. V. Hill, A discussion on muscular contraction and relaxation: Their physical and chemical basis, Proc. Roy. Soc. (London) B137, 40 (1950).

6. L. Stark, Biological organization of the control system for movement, Quarterly Progress Report No. 61, Research Laboratory of Electronics, M. I. T. , April 15, 1961, pp. 234-238; cf. Fig. XIV-22.

7. A. V. Hill, The Dimensions of Animals and Their Muscular Dynamics, Lecture to Royal Institution of Great Britain, London, November 4, 1949.

B. TRANSIENT RESPONSES OF HUMAN MOTOR COORDINATION SYSTEM

1. Instrumentation

A method of measuring the rotation of the wrist of a human subject has been developed to further investigate the muscle coordination system in man.   This light-coordination machine (LCM) has the advantage of having very low friction and inertia that act as constant feedback terms and therefore alters the mechanical dynamics of the human arm only slightly.

The light-coordination machine employs a linear display of both target input and

angular position of the handle. A specially designed mirror galvanometer manu-
factured by the Sanborn Company to the specifications of L. Young and H. Hermann is
used to control the position of the input target — a slit of light on a transluscent screen.
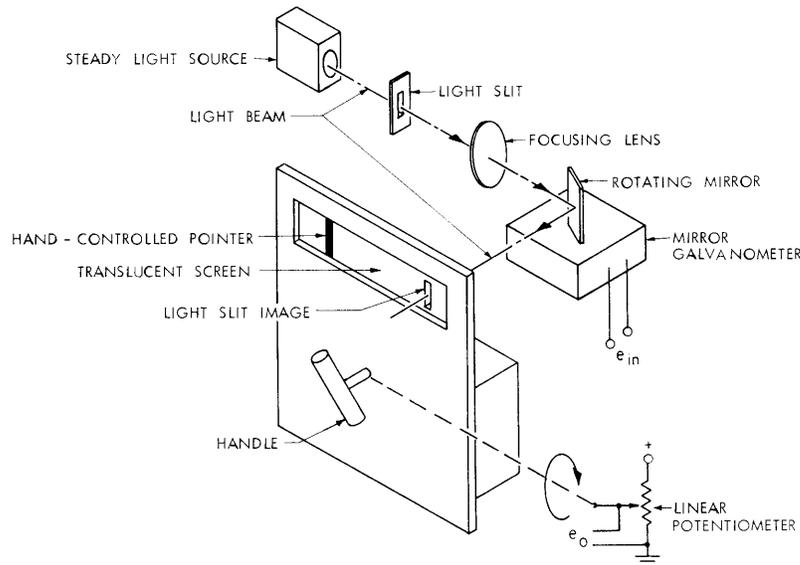Figure XXVIII-6 is a pictorial representation of the complete system. The mirror

Fig. XXVIII-6. Pictorial diagram of the light-coordination machine.

galvanometer and associated dc driver amplifier has variable sensitivity and is linear
over a range of ±25° of target position. A linearity calibration curve is shown in
Fig. XXVIII-7 and a frequency-response curve in Fig. XXVIII-8. The frequency
response is flat up to 80 cps when the LCM is set for critical damping.

The subject is isolated by a black curtain from external light and distractions caused
by the experimenter. The subject is instructed to follow the target (a 0.1 × 1.0-cm
strip of light) with the pointer that he controls by the rotation of his wrist. Input-driving
signals are generated by analog-function generators. The inputs and outputs are recorded
on a portable Sanborn recorder as shown in Fig. XXVIII-9.

2. Experiment

The responses of the human motor coordination system to impulses and regular and
irregular square waves of target position were studied with the LCM.

a. Response to a Square-Wave Input

The response of the wrist to an input composed of irregular steps of position is
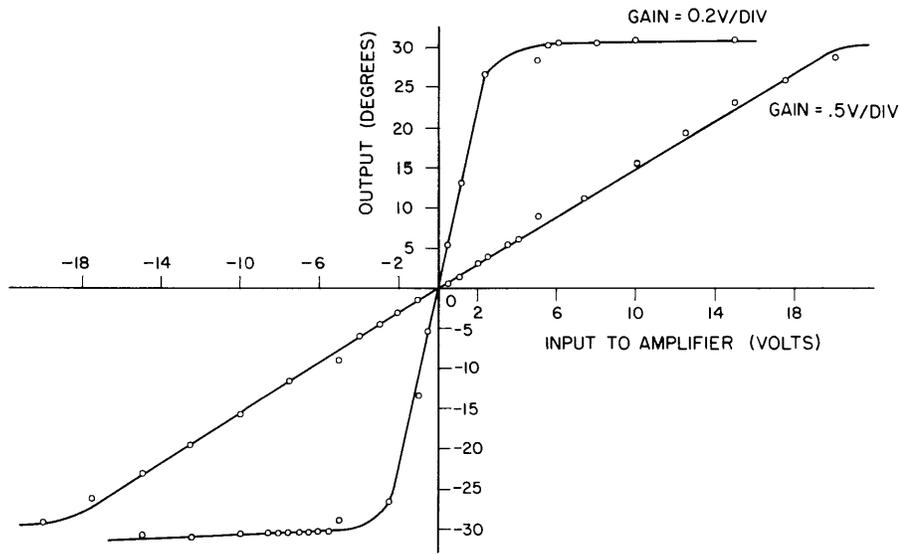shown in Fig. XXVIII-10a. This input had four step amplitude levels, a pattern-repetition

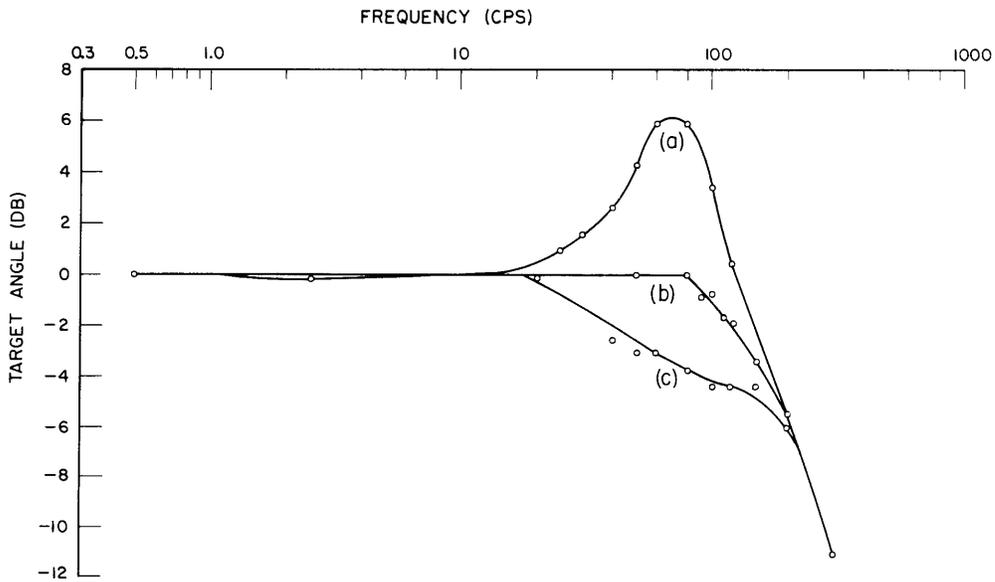Fig. XXVIII-7. Linearity calibration of the light-coordination machine.

Fig. XXVIII-8. Frequency-response calibration of light galvanometer and amplifier. The target angle amplitude in decibels vs frequency in cps is shown with damping ratio as a parameter: (a) underdamped; (b) critically damped; (c) overdamped. The experiments are run with the apparatus adjusted for condition (b).
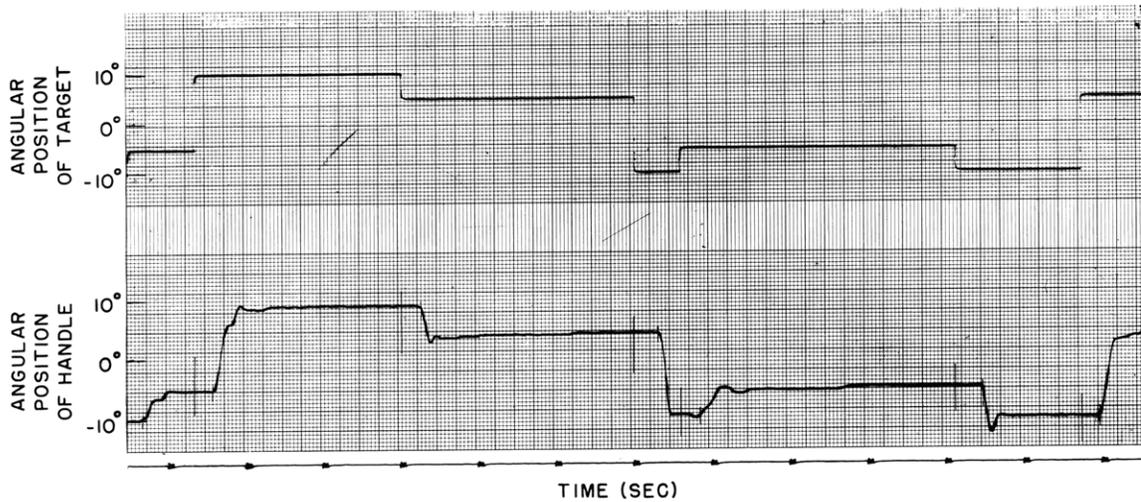
317

Fig. XXVIII-9. Sample input-output of the light coordination machine. Top trace, input target position vs time; lower trace, the subject's response to this input vs time. The pencil marks are part of the analysis procedure.

period of 60 seconds, and 27 steps per period. The length of the steps varied between 120 msec and 3 seconds and their distribution was approximately flat. The long pattern period made this input look unpredictable to the subject. The distribution of response delay to this irregular input is shown in Fig. XXVIII-11a. Time delay is the period between onset of target motion and onset of hand motion. The minimum time delay is 150 msec, and the median time delay is 250 msec.

Regular sequences of square waves and responses to them are shown in Figs. XXVIII-10b, c, d, e, and f. Because of the regularity of target motion, the subject could predict it and could move his handle pointer either in synchrony with target motion, ahead of target motion, or behind target motion, but with a time delay shorter than that found in the response to an irregular square wave. Figure XXVIII-10c shows a sample of such responses, and Fig. XXVIII-11c shows a histogram of time delays. Here it can be clearly seen that all of the responses represented predictions. Prediction is defined as a response that starts within ±150 msec of the input. The input is considered to start at time zero. Figure XXVIII-10b and 10e shows better responses to regular sequences at slower frequencies. It is interesting that even though the subject knew that the input was repetitive and predictable, he made little attempt to predict. This result is also shown in Fig. XXVIII-11b in which a histogram of reaction time delays to the 0.5-cps regular input is shown.

With square waves of very high repetition rates, as shown in Figs. XXVIII-10d and XXVIII-11d, the subject, although at the limit of his performance, was still able to predict. In fact, overprediction sometimes occurred. By "overprediction" we mean that the subject, after allowing for the time of actual movement of the hand, may be in
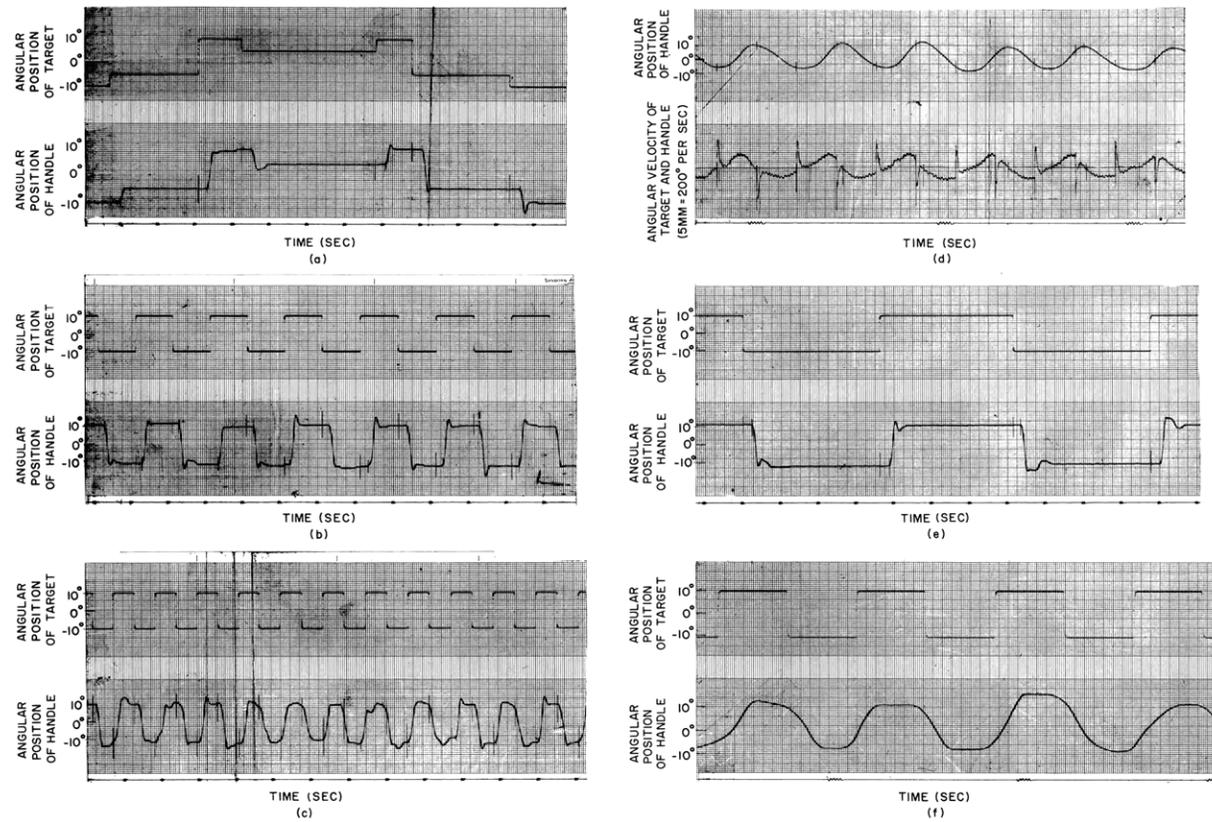
Fig. XXVIII-10. Records of wrist movements during tracking of regular and irregular square waves. Top trace in (a), (b), (c), (e), and (f), input; lower trace, response. Top trace in (d), output; lower trace, derivative of the input and derivative of the output. (a) Irregular steps. (b) Square wave at 0.5 cps; (c) square wave at 1.3 cps; (d) square wave at 2.5 cps; (e) square wave at 0.15 cps; (f) square wave at 1.0 cps.
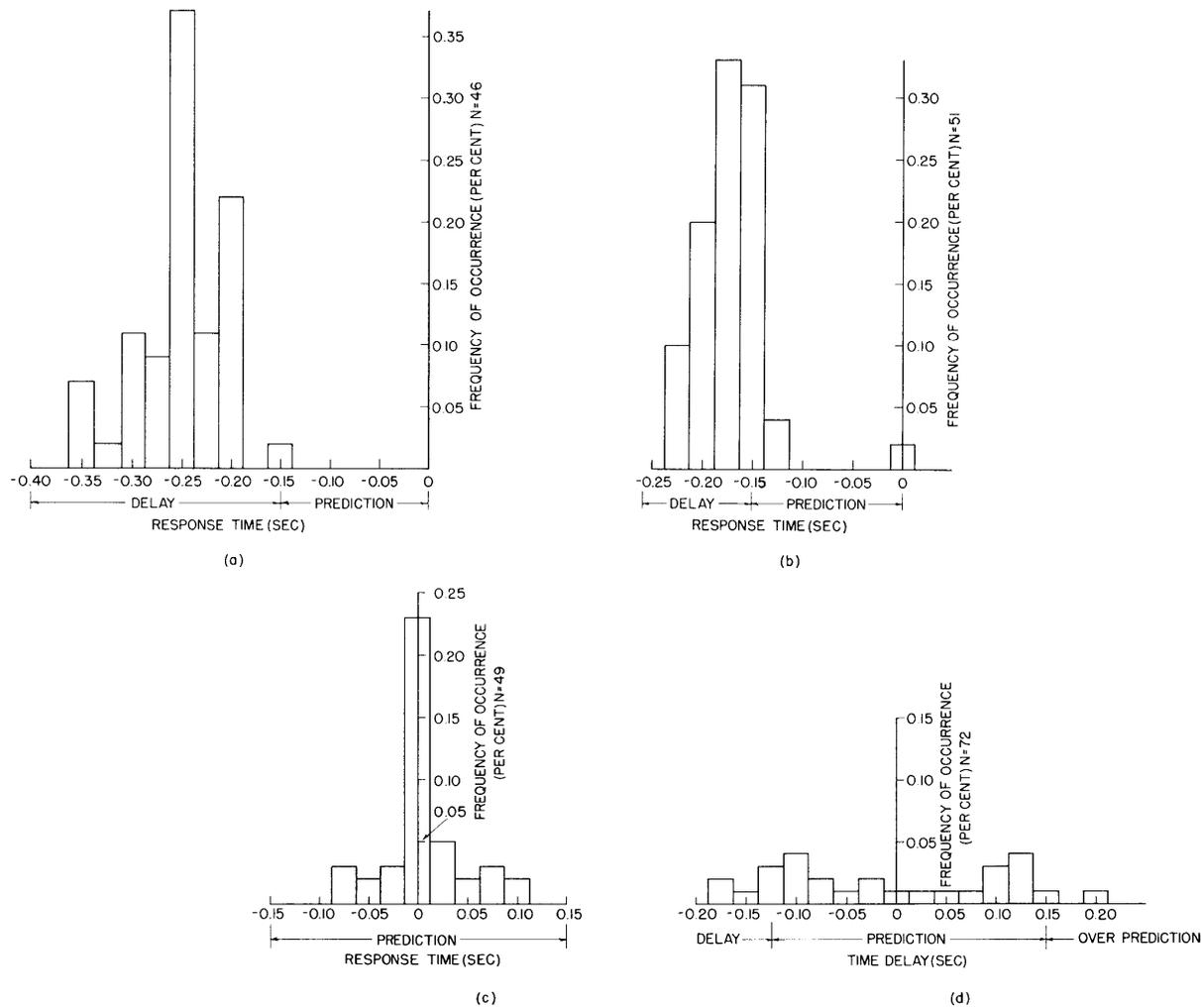
Fig. XXVIII-11. Histograms of response delay times during tracking of regular and irregular square waves. (a) Irregular wave; (b) square wave at 0.5 cps; (c) square wave at 1.3 cps; (d) square wave at 2.5 cps. An example of the bimodal distributions that occur for high input frequencies is shown in (d). Distributions of response time delays for different square-wave inputs are shown as histograms of the per cent of responses occurring at each time delay. N is total number of responses. Bar width indicates the response time delays lumped together.
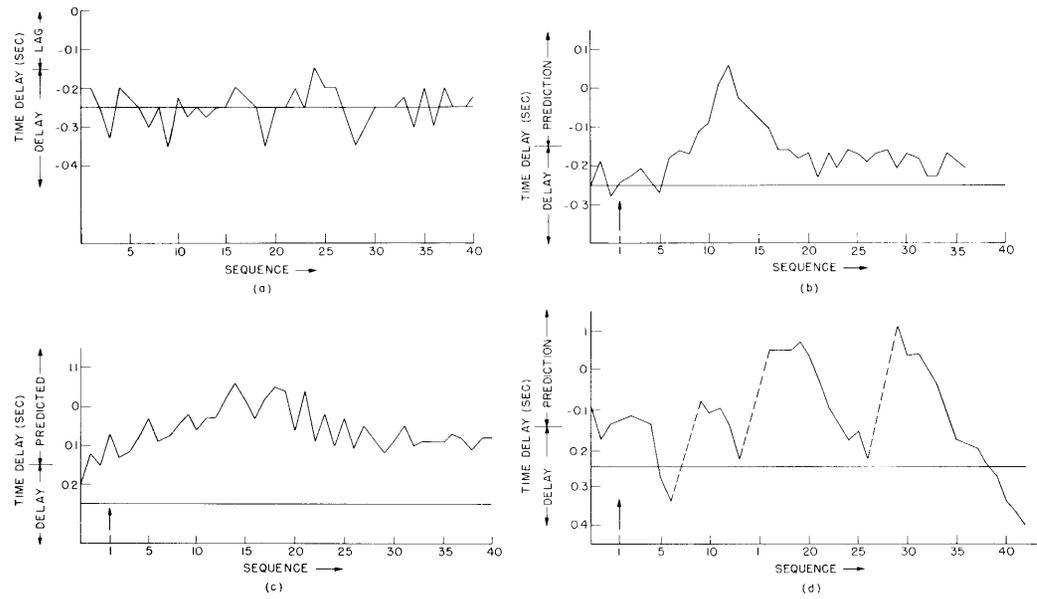
Fig. **XXVIII**-12. Sequential patterns of response time delays and predictions to regular and irregular square waves. Arrow indicates first response to a reqular square wave after a long series of responses to irregular square waves. The median time delay for responses to irregular square waves is indicated on each figure for comparison. The dashed lines indicate that responses were skipped. (a) Irregular steps; (b) square waves at 0.5 cps; (c) square waves at 1.3 cps; (d) square waves at 2.5 cps.

a new position and awaiting the target before the target itself has arrived. We call pre-
dictions greater than 150 msec overprediction, since this seems to be the time required
for moving the hand from one position to a new position 20° away. It is very interesting
to note that overprediction is a much less prominent phenomenon in hand movement than
in eye movement.[1] However, the reasons for this are still not clear to us.

At these high repetition rates a special display technique, shown in Fig. XXVIII-10d,
is used to make our experimental measurements more precise. The derivative of target
motion is superimposed on the derivative of hand motion. This method enables us to
determine time delays more precisely.

The sequential patterns of response time delays and predictions for typical square-
wave inputs are displayed in Fig. XXVIII-12. This figure shows the development of pre-
dictive responses as the subject ascertains the regular pattern of square-wave target
motion. Figure XXVIII-12b and 12c shows the development of prediction and ultimate
leveling at a median response time in the delay and prediction ranges. Figure XXVIII-12d
shows an example of consistent behavior obtained at frequencies of approximately
2.5 cps. There is no clear-cut development of predictive response, and indeed the
entire response pattern is really a series of transient phases in which the subject gradu-
ally goes from prediction toward delay, realizes his error, and actually skips a response
or two in order to again apply prediction. It is also of interest to note both the short-
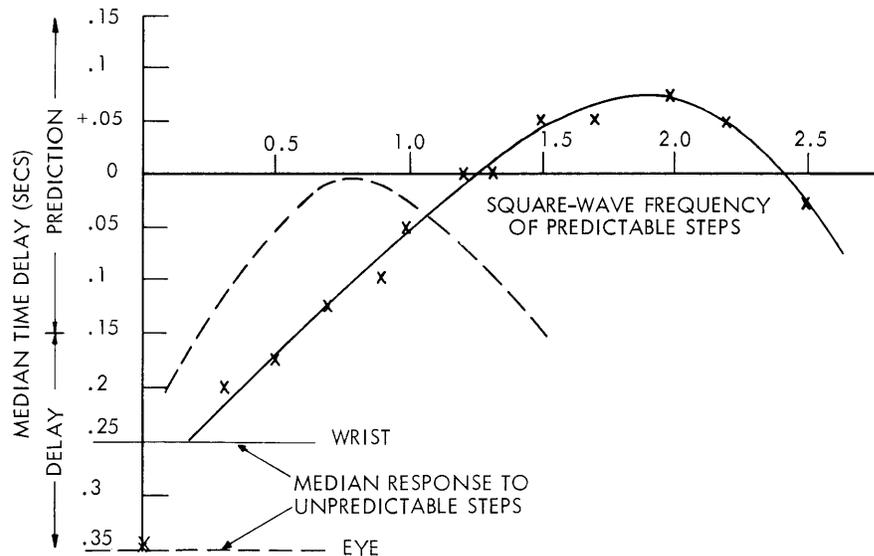and long-term variability of responses.

Fig. XXVIII-13. Wrist- and eye-movement response delay times as a function of fre-
quency of regular square waves. Solid line represents wrist move-
ment and the dashed line represents eye movement. The average
response time delay to unpredictable square waves as input is also
shown for both movements.

Figure XXVIII-13 summarizes the results of a number of these experiments. The median time delay is plotted as a function of the frequency of the regular square-wave inputs. This curve does not show the widest possible range of individual time delays, which is from 3.5 sec delay to 0.20 sec overprediction. The curve of the function in Fig. XXVIII-13 shows prediction occurring in the middle-frequency area and lack of prediction in the slow- and high-frequency areas. The median response to irregular square waves is indicated for comparison. The dashed curve represents the median responses of the similar eye-movement tracking experiment.[1] It should be noted that the hand system can operate in a higher frequency range than the eye-movement system. Thus, it is clear that eye tracking is not limiting hand tracking. Observation of the subject's eyes during hand tracking indicates that eye movement occurs when the hand is tracking a target motion of 1.3 cps. However, the hand is still able to track at 2.5 cps, while the eye appears stationary.

In summary, the experiments reported above describe the behavior of the hand in tracking regular and irregular square waves. The response differences to these two experimental conditions show the necessity of controlling this aspect of the input function. Similarities and differences in hand tracking as compared with eye tracking are quantitatively discussed.

b. Response to an Impulse Input

In this experiment an impulse signal of 20° amplitude is projected upon the translucent screen at irregular intervals. Only one direction of wrist rotation was studied, that of supination. The subject was instructed to set his arm, wrist, and hand muscles in either a "relaxed," "moderately tense" or "very tense" state and then respond to target movement, and to maintain that muscle state until instructed to change. Since most subjects feel that they can retain the relaxed and moderately tense states for only a short period of time before changing the state, they are requested to retain one state of tension for not more than from 30 to 40 seconds. In Fig. XXVIII-14a, 14b, and 14c are shown records of the subject's response to an impulse input with muscles in each of the three states of tension.

The following variables were considered in the analysis of the response:

(i) amplitude ratio: amplitude output/amplitude input,

(ii) time delay (T_d): time from the onset of target movement to the onset of wrist movement,

(iii) time to peak (t_p): time from the onset of wrist movement to point of maximum amplitude of the first peak of response,

(iv) time k (t_k): time from the kth peak of response to the $(k+1)^{th}$ peak of response,

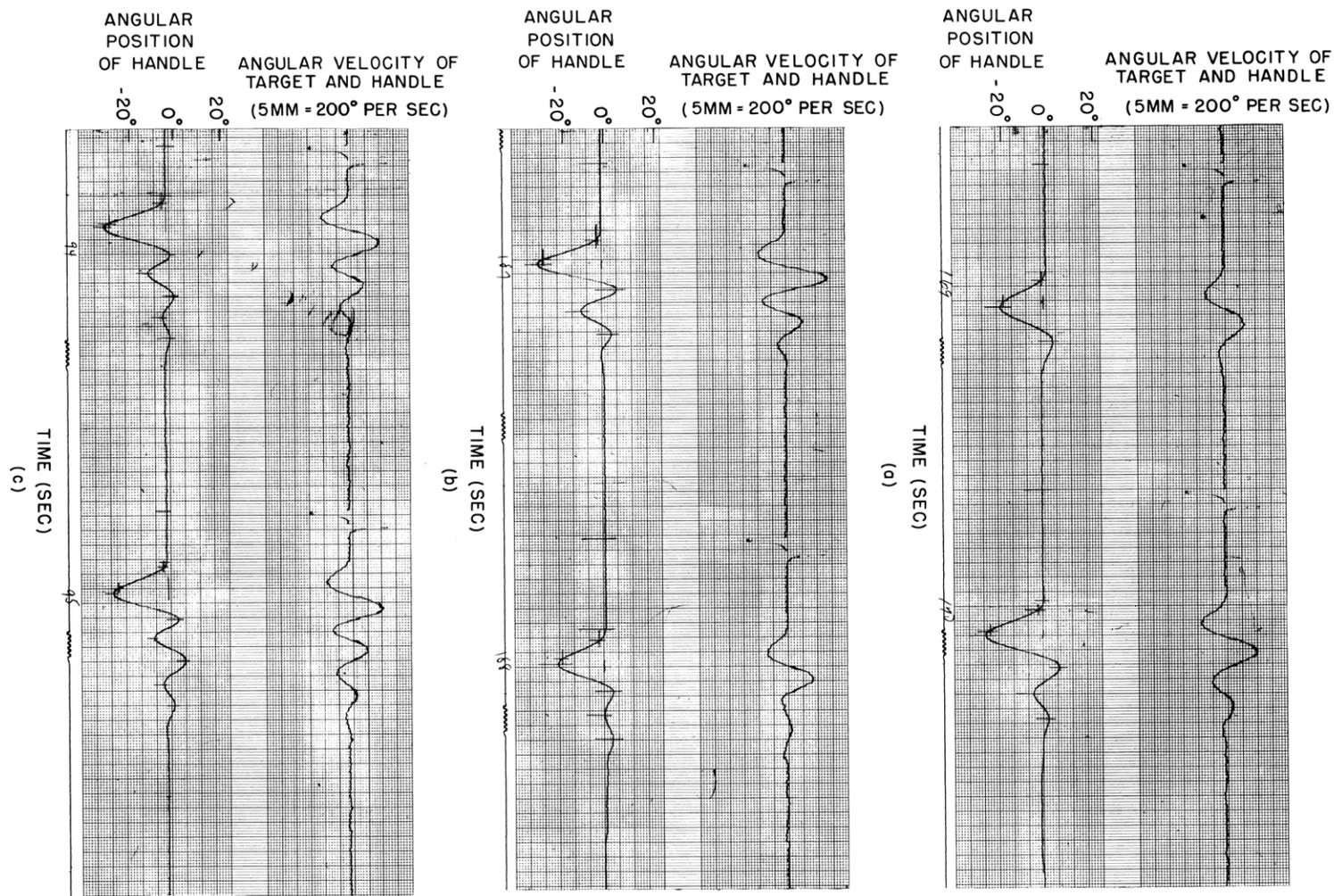(v) time 19 (t_{19}): a measurement similar to that of the rise time in the response

Fig. XXVIII-14. Record of wrist movements in response to an impulse input with three different states of muscle tension: (a) relaxed condition; (b) moderately tensed condition; (c) very tense condition.

to a step input; that is, the time from the point at which the first peak in response reaches 10 per cent of input amplitude to the point at which the response reaches 90 per cent of input amplitude,

(vi) number of ringing cycles (not including first cycle) until the response has stabilized at zero level, and

(vii) ringing frequency: average frequency of oscillation of ringing cycles until response has leveled to zero.
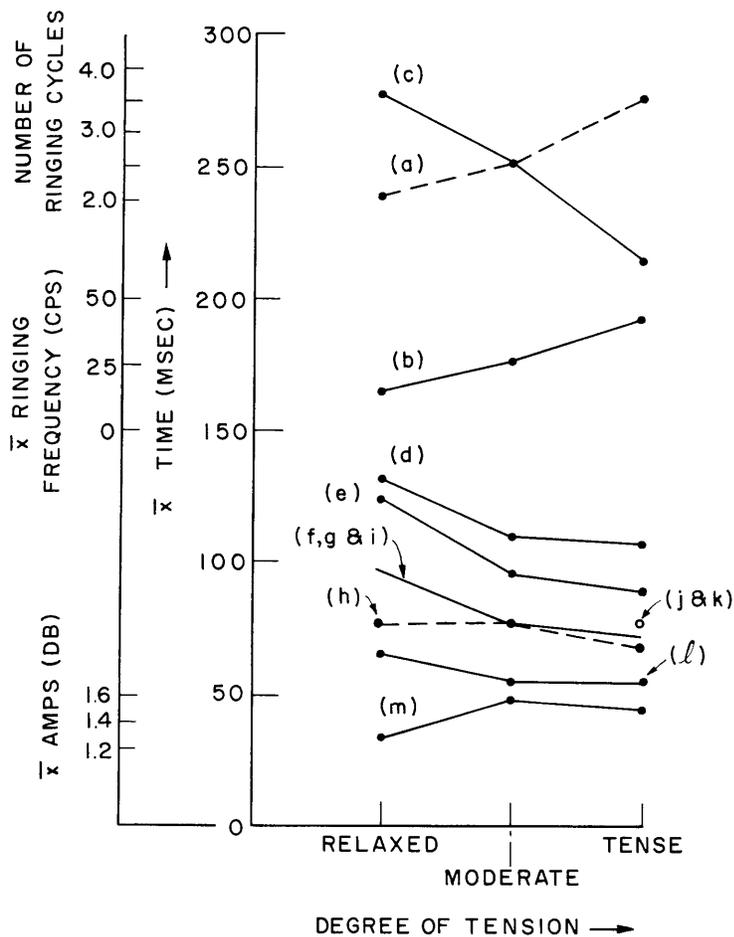

Fig. XXVIII-15. A plot of variables analyzed in the response to an impulse input as a function of state of muscle tension: (a) number of oscillations; (b) average ringing frequency; (c) average response time delay, (t_d); (d) average time to peak, (t_p); (e) average t_1; (f) average t_2; (g) average t_3; (h) average t_4; (i) average t_5 (no data for relaxed point); (j) t_6 (one point); (k) t_7 (one point); (l) average t_{19}; (m) average amplitude ratio in decibels. For simplification, (f), (g), and (i) have been superimposed, since their graphs lay almost on top of each other; the same was done for (j) and (k).

325

In Fig. XXVIII-15 the average at each state of tension of the above variables is plotted as a function of the state of tension. The following relations seem evident: (a) amplitude ratio does not seem to vary as a function of degree of tension; (b) t_d, t_p, t_k, and t_{19} seem to show a decrease as the degree of tension increases, and (c) the number of ringing cycles and the ringing frequency increase as degree of tension increases.

In summary, the response occurs in two parts: the first response cycle is the attempt by the subject to reproduce the impulse; the second part consists of the ringing cycles. Both constitute a response whose characteristic is strongly related to the physiological degree of muscle tension of the subject. There seems to be no limitation of the adequacy (gain and temporal characteristics) of voluntary movement by the preset degree of tension under these experimental conditions; this is quite different from the effect of maintained tension on freewheeling frequency as discussed earlier.[2,3]

<div style="text-align:center">J. Houk, Y. Okabe, Helen E. Rhodes, L. Stark, P. A. Willis</div>

References

1. L. Stark, G. Vossius, and L. R. Young, Predictive control of eye movements, Quarterly Progress Report No. 62, Research Laboratory of Electronics, M. I. T., July 15, 1961, pp. 271-281.

2. L. Stark and M. Iida, Dynamical response of the movement coordination system of patients with Parkinson syndrome, Quarterly Progress Report No. 63, Research Laboratory of Electronics, M. I. T., October 15, 1961, pp. 204-213.

3. L. Stark, Neurological organization of the control system for movement, Quarterly Progress Report No. 61, Research Laboratory of Electronics, M. I. T., April 15, 1961, pp. 234-238.

C. OPTOKINETIC NYSTAGMUS

Optokinetic nystagmus is a periodic response to a rapidly moving visual field. It is sometimes called "train nystagmus," because of its occurrence when one is gazing from a train window. It is an involuntary reflex that has been used to disprove feigned blindness in man, and to measure visual acuity and visual sensitivity in animals.

We have adapted our eye-position experimental apparatus, described in Quarterly Progress Report No. 62 (pages 268-270), to study this intriguing phenomenon, as shown in Fig. XXVIII-16. A television cathode-ray tube is driven by pulse generators to produce a pattern of moving stripes across the monitor face that is rotated 90° to take advantage of the slower vertical frame rate. Shintaro Asano was most helpful in the development of this stimulating unit. The striped pattern can be varied easily as to number, velocity, width, and intensity of the stripes. An objective record of these parameters is obtained by monitoring the screen pattern with a phototransistor.

When the stripes move slowly enough, the subject can track them from one side of
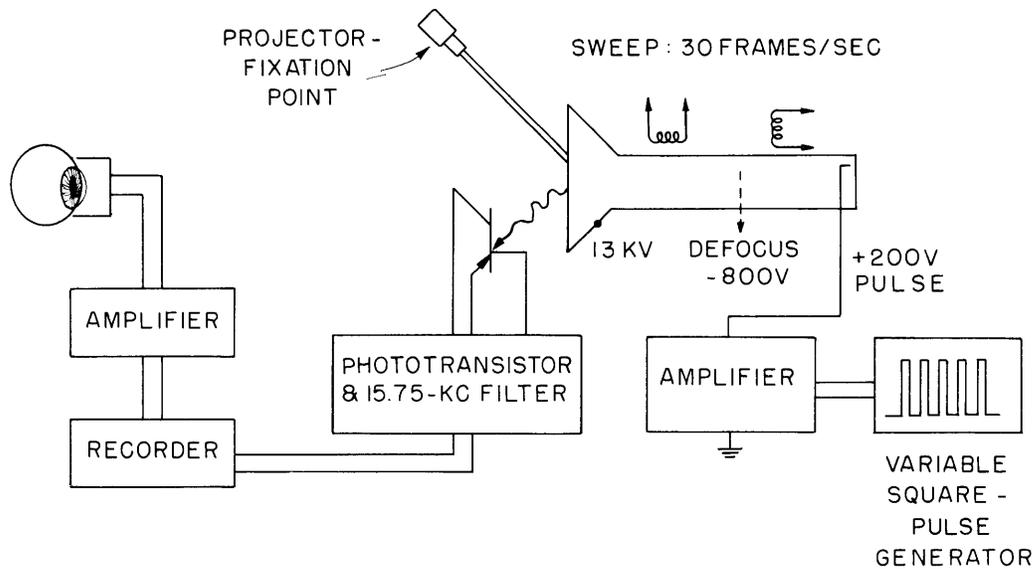
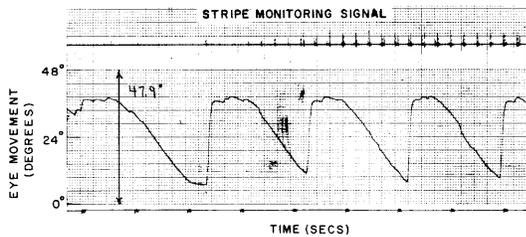Fig. XXVIII-16. Diagrammatic sketch of experimental arrangement.

Fig. XXVIII-17. Calibration run showing monitor-generated signal for each passage of stripe. Note the smooth pursuit movement of the eye at 24° per second.
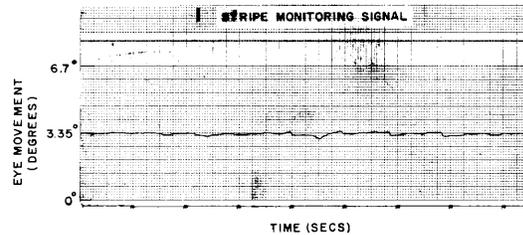

Fig. XXVIII-18. Record showing ability of the subject to maintain fixation when there is no moving stripe pattern.
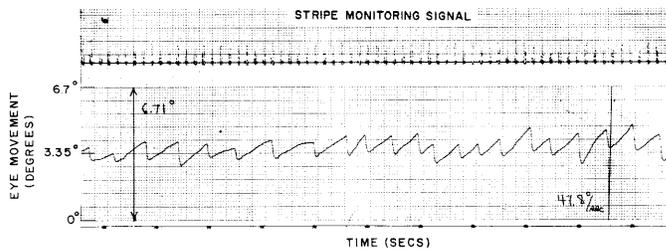

Fig. XXVIII-19. Record showing involuntary optokinetic nystagmus when the stripe pattern passes across the screen at 48° per second, and thus compensates for approximately 4 per cent of the retinal image velocity. Note the saccadic phase of the nystagmus.

the visual field to the other, as shown in Fig. XXVIII-17. This serves as a calibration for linearity of the experimental system.

A fixation point is established on the face of the screen, and the subject attempts to maintain a steady gaze. Without the moving pattern of stripes, accurate fixation is possible, as shown in Fig. XXVIII-18. When a striped pattern with a velocity of 47.8 degrees per second is put on, this conflicts with the steady fixation. Optokinetic nystagmus is produced and appears as the irregularly repetitive saw-toothed waveform shown in Fig. XXVIII-19. The slower tracking phase is to be contrasted with the rapid saccadic return movement. It is important to clearly understand that the tracking phase has a velocity of only approximately 4 per cent of the stripe velocity. Therefore little compensation for relative velocity of retinal image and retina occurs. Also, limitation in the physical range of eyeball movement is not the stimulus for the return saccadic jump.

L. Stark, G. Nelson